Parametric Analysis Applied to the Geometric Optimization of Filtered Iron Ore Tailings Stacks

Kevyn Douglas Dias Silva[a,*]; Michel Melo Oliveira[a]; Eduardo José Diniz[b]

a Department of Mining Engineering, School of Engineering, Universidade Federal de Minas Gerais (UFMG), Av. Antônio Carlos 6627, Pampulha, Belo Horizonte, MG, 31270-901, Brazil

b Check Slope, Minas Gerais, Brazil

* Corresponding author: kevynddiasm@gmail.com

Keywords

iron ore tailings; dry stacking; slope stability; parametric analysis; factor of safety; limit equilibrium; ABNT NBR 13028-3

Declarations

Conflict of interest: The authors declare no competing interests.

Funding: This research received no specific grant from any funding agency.

Data availability: The numerical data supporting the findings of this study are reported in full in Tables 5 to 7 of this manuscript. Model files are available from the corresponding author upon reasonable request.

Abstract

The high iron ore output in Brazil and the regulatory restrictions imposed on tailings dams after the Mariana (2015) and Brumadinho (2019) failures have accelerated the adoption of dry stacking of dewatered tailings. This work develops a parametric analysis for the geometric optimization of filtered iron ore tailings stacks, assessing the influence of slope angle, berm width and bench height on the factor of safety (FS) and the storable volume, in accordance with ABNT NBR 13028-3:2025. Three-dimensional modeling and volume estimation were performed in Micromine, and stability analyses in Slide2, using the Morgenstern-Price limit equilibrium method under drained conditions with effective-stress parameters. The study was carried out in two stages: Stage I used reference parameters compiled from the literature for filtered and compacted tailings from the Iron Quadrangle ($\varphi' = 33°$, $c' = 0$ kPa, $\gamma = 22$ kN/m³), and Stage II applied the methodology to the topography and laboratory parameters of an actual operation ($\varphi' = 32°$, $c' = 0$ kPa, $\gamma = 19.8$ kN/m³). Results show that the slope angle is the governing geometric parameter for FS, with limiting angles of 23° (Stage I) and 24° (Stage II) for the FS ≥ 1.50 criterion; berm width has no measurable effect on global stability (FS coefficient of variation below 1.1%), acting only to reduce volume; and bench height yields an FS that converges asymptotically to the value governed by the individual slope inclination beyond a threshold ($H \approx 6.5$ m in Stage I). It is concluded that geometric design should fix the slope angle at the regulatory limit and optimize berm width and bench height solely as a function of storable volume.

1. Introduction

Iron ore is the leading product of Brazilian mining in terms of output volume. In 2023, national beneficiated iron ore production reached approximately 437 million tonnes at an average grade of 62.7% Fe, concentrated in the states of Minas Gerais and Pará (ANM, 2024; IBRAM, 2024), placing Brazil among the largest global producers of this commodity. The magnitude of this output implies a proportionally high generation of tailings from mineral processing, particularly from concentration circuits that produce fine fractions with no commercial value. Iron ore is the single largest contributor to mining tailings generation in the country, accounting for approximately 35% of the total, and the overall tailings generation in Brazil is estimated to exceed 680 million tonnes by 2030 (ANM, 2024).

Tailings management moved to the centre of mining engineering practice after the failures of the Fundão dam in Mariana (2015) and of the Córrego do Feijão mine dam in Brumadinho (2019), which resulted in social, environmental and regulatory impacts of considerable magnitude. In response, Federal Law 14.066/2020 amended the Brazilian National Dam Safety Policy and prohibited the construction or raising of mining tailings dams by the upstream method (Brasil, 2020). Resolution ANM 95/2022 subsequently consolidated regulatory measures specific to mining dams, reinforcing directives associated with the safety of these structures (ANM, 2022).

Although these instruments address dams directly, the resulting institutional environment has driven the adoption of technical alternatives with reduced dependence on large hydraulic reservoirs. Prominent among these alternatives is the disposal of previously dewatered tailings in stacks. The normative consolidation of this disposal method occurred with the publication of the fifth edition of ABNT NBR 13028 on 4 December 2025, structured in three parts: NBR 13028-1 (terminology), NBR 13028-2 (general design requirements) and NBR 13028-3, specific to the disposal of dewatered tailings in stacks (ABNT, 2025a, 2025b, 2025c). Part 3 establishes criteria related to the geotechnical characterization of the material, geometric definition, drainage control and verification of global stability.

Because dewatered iron ore tailings exhibit predominantly frictional behaviour, the physical configuration of the stack directly influences the factor of safety obtained in limit equilibrium stability analyses (Morgenstern and Price, 1965; Duncan et al., 2014). In mine areas, where the available footprint is constrained by physical and operational conditions, the maximization of storable volume must be compatible with minimum stability criteria. The trade-off between capacity and safety is therefore a geometric optimization problem, yet the relative contribution of each geometric parameter to the factor of safety of filtered tailings stacks has not been systematically quantified for the conditions prevailing in the Iron Quadrangle.

This paper addresses that gap by developing a parametric analysis applied to dewatered iron ore tailings stacks, assessing the influence of slope angle, berm width and bench height on both the factor of safety and the accumulated volume, in accordance with ABNT NBR 13028-3:2025. Three-dimensional modeling and volume estimation were performed in Micromine, while stability analyses were conducted in Slide2 using the Morgenstern-Price limit equilibrium method with automatic search for the critical slip surface by means of the Auto Refine Search algorithm applied to circular surfaces. Analyses were carried out under drained conditions, with strength parameters expressed in terms of effective stresses and the material modelled as homogeneous and isotropic, a hypothesis consistent with the compacted, low-plasticity nature of filtered tailings.

Beyond the initial application to an area delimited by a predefined physical boundary, the methodology is applied to a second topography associated with an operating iron ore project, using geotechnical parameters determined specifically for that material. This second stage allows the consistency of the results to be assessed against simultaneous variations in geometric conditions and material properties, and therefore establishes whether the identified trends are governed exclusively by geometry or also by the strength parameters of the tailings.

2. Background

2.1 Geotechnical properties of iron ore tailings

From a geotechnical standpoint, iron ore tailings exhibit predominantly frictional behaviour, with the effective friction angle (φ') as the main parameter governing shear strength, while the effective cohesion (c') tends to be small or negligible (Lopes, 2000; Hernandez, 2002). Experimental studies show that these materials, although frequently classified by grain size as low-plasticity silts, behave analogously to fine sands when subjected to higher density conditions, particularly in the case of filter-dewatered and compacted tailings (Carvalho et al., 2024; Pereira, 2024).

Table 1 compiles the shear strength parameters determined by triaxial (CID and CIU) and direct shear tests reported in the national and international literature for iron ore tailings, with emphasis on studies carried out in the Iron Quadrangle (IQ), the region of greatest relevance to the present work.

Table 1. Shear strength parameters (φ' and c') and natural unit weight (γ) of iron ore tailings reported in the literature. IQ = Iron Quadrangle; CID = isotropically consolidated drained triaxial test; CIU = isotropically consolidated undrained triaxial test; NR = not reported.

Reference	Origin	Tailings type	Test	φ' (°)	c' (kPa)	γ (kN/m³)
Espósito (2000)	Xingu and Monjolo, MG	Fine silty	CID triaxial	28–35	0–5	NR
Lopes (2000)	IQ, MG	Fine to sandy	CID triaxial	30–42	≈ 0	NR
Presotti (2002)	IQ, MG	Variable Fe grade	CID triaxial	28–40 *	≈ 0	NR
Hernandez (2002)	IQ, MG (4 dams)	Mixed (fine/coarse)	CID triaxial	26–45	≈ 0	NR

Reference	Origin	Tailings type	Test	φ' (°)	c' (kPa)	γ (kN/m³)
Ferrante et al. (2016)	IQ, MG (Stack 2A)	Compacted sandy-clayey silt (RC = 98% SP)	CID/CIU	32 **	14 **	24.0 **
Morgenstern et al. (2016)	Fundão dam, MG	Sandy	CID triaxial	28–37	≈ 0	NR
Barbosa (2022)	MG (filtered, 161 m)	Filtered, compacted	CIU triaxial	30–38	0–10	NR
Fontes et al. (2023)	Belo Horizonte, MG (co-disposal)	Filtered sandy silt	CID triaxial	31.5	1.2	22.0
Carvalho et al. (2024) – IOT_A	IQ, MG (filtered)	Filtered, compacted	CID triaxial	33.9	< 5	NR
Carvalho et al. (2024) – IOT_B	IQ, MG (filtered)	Filtered, compacted	CID triaxial	32.8	< 5	NR
Coelho and Camacho (2024)	Portugal (Moncorvo)	Sandy silt (Gs ≈ 4.7)	CIU triaxial	42 ***	≈ 0	≈ 29 ****
Pereira (2024)	IQ, MG (Pico mine, filtered)	Filtered, compacted	Direct shear	32.8–36.0 *****	21–62 *****	NR
Adopted – Stage I	Compiled literature (n = 11)	Parametric reference	–	33	0	22
CI&A Lab (2022) – Stage II	MG (magnetic separation)	Compacted silty	CIU triaxial	32	≈ 0	19.8

** Presotti (2002): φ' ranges from approximately 28° to 40° depending on iron content and void ratio. ** Ferrante et al. (2016): values refer to the Stack 2A fill compacted to RC = 98% of Standard Proctor; the loose tailings from the dam exhibit φ' = 30°, c' = 2 kPa and γ = 19 kN/m³. *** Coelho and Camacho (2024): the elevated value is attributed to particle angularity and Gs ≈ 4.7, and is not representative of the IQ. **** γd,max = 2.99 g/cm³ obtained under Modified Proctor with an atypically high Gs; not adopted as a reference for the IQ. ***** Pereira (2024): direct shear tests (ASTM D3080) on submerged specimens of blend C at relative compaction between 97% and 103% and moisture deviations of ±2%; φ' = 34.4° ± 1.2°. The cohesion intercepts of 21 to 62 kPa are attributed by the author to the dilatancy of the densely compacted specimens and should not be interpreted as true cohesion; c' = 0 kPa is therefore retained as the conservative reference for this material class.*

The compiled data show that the effective friction angle of iron ore tailings varies broadly between 26° and 45°, an interval that reflects the diversity of grain size distributions, void ratios, iron contents and compaction conditions considered across the different investigations (Lopes, 2000; Hernandez, 2002; Presotti, 2002). When the analysis is restricted to studies on filtered and compacted tailings from the Iron Quadrangle, the condition directly applicable to dry stacking, good convergence of the strength parameters is observed. Barbosa (2022), who tested the material at different degrees of compaction, reports effective friction angles ranging from 30° to 38°, a range that encompasses the point values determined in the remaining studies from the region, between 31.5° (Fontes et al., 2023) and 34.4° ± 1.2° (Pereira, 2024), with intermediate values of 32.8° and 33.9° (Carvalho et al., 2024).

Statistical treatment of the compiled φ' values, excluding the result of Coelho and Camacho (2024) on the grounds that it originates from a Portuguese mine with an atypically high specific gravity (Gs ≈ 4.7) and is not representative of the geological context of the IQ, yields a mean of 33.5° and a standard deviation of 1.5° for the eleven remaining values. The subset composed exclusively of studies on filtered and compacted tailings from the IQ (n = 5) has a mean of 33.3° and a standard deviation of 1.2°, reinforcing the convergence of values in the 32° to 36° range. Effective cohesion is null or near-null in most studies of non-plastic silty tailings produced by physical separation, a behaviour consistent with the absence of interparticle cementation and with the predominantly silty grain size of these materials (Lopes, 2000; Hernandez, 2002; Morgenstern et al., 2016; Fontes et al., 2023). Where a non-zero cohesion intercept is reported for these materials, as in Pereira (2024), it is attributed to dilatancy of

densely compacted specimens rather than to interparticle bonding, and is therefore not carried into design.

The natural unit weight (γ) is a fundamental input parameter in limit equilibrium analyses, since it determines the weight of each slice in the Morgenstern-Price formulation (Duncan et al., 2014). Iron ore tailings exhibit Gs typically between 3.0 and 4.7 g/cm³ owing to the presence of iron oxides such as hematite and magnetite, resulting in natural unit weights higher than those of conventional soils. For filtered tailings compacted at Standard Proctor energy to between 93% and 97% relative compaction, values reported in the literature fall in the range of 19.0 to 24.0 kN/m³ (Table 2).

Table 2. Compaction parameters and natural unit weight of filtered and compacted iron ore tailings compiled from the literature. SP = Standard Proctor; MP = Modified Proctor.

Reference	Origin	Gs (g/cm³)	γd,max (g/cm³)	w,opt (%)	γnat ref. (kN/m³)	Energy
Ferrante et al. (2016) – Stack 2A	IQ, MG	3.701	2.069 (RC = 98% SP)	11	24.0	SP
Consoli et al. (2022)	IQ, MG	≈ 3.4	1.70–1.90	11.6	20.0–21.5	SP
Barbosa (2022)	MG (filtered)	≈ 3.5	1.90–2.10	≈ 12	21.3–23.5	SP / MP
Fontes et al. (2023)	MG (co-disposal)	3.47	2.00	12.7	22.0	SP
Pereira (2024)	IQ, MG (Pico mine, filtered)	3.08–3.35	1.87–1.95	10.6–11.5	NR	SP
Coelho and Camacho (2024)	Portugal (high Gs)	4.70	2.99	8.95	≈ 29.3	MP
CI&A Lab (2022) – Stage II	MG (magnetic separation)	3.348	2.069	14.9	19.8	SP
Adopted – Stage I	IQ filtered literature	≈ 3.2–3.5	≈ 1.95–2.05	≈ 11–13	22.0	SP (95%)

On the basis of this compilation, the reference parameters adopted for the parametric analysis of Stage I are an effective friction angle φ' = 33°, an effective cohesion intercept c' = 0 kPa and a natural unit weight γ = 22 kN/m³. The adopted φ' = 33° is a conservative reference value. It lies below the central tendency of both the subset of filtered and compacted tailings from the Iron Quadrangle (mean 33.3°, standard deviation 1.2°) and the full compiled sample (mean 33.5°, standard deviation 1.5°), and it sits within the lower half of the μ ± σ band of both sets. It is also lower than every point value reported for filtered and compacted IQ tailings except that of Fontes et al. (2023), and 1.4° below the mean reported by Pereira (2024) for the same material class. The choice of c' = 0 kPa compounds this conservatism, since several of the compiled studies report a positive cohesion intercept for compacted specimens. Because the factor of safety of a purely frictional slope increases monotonically with φ', adopting a friction angle below the central tendency of the reference population ensures that the limiting angles identified in Stage I are lower bounds rather than best estimates.

2.2 Limit equilibrium analysis

The stability of tailings stacks is directly related to the shear strength of the material, the geometry of the structure and the drainage conditions. In structures composed of granular or partially saturated materials, mechanical behaviour is strongly influenced by the effective stress state (Fredlund and Rahardjo, 1993).

Stability is usually assessed by limit equilibrium methods, which compare the resisting forces mobilized by the shear strength of the material along a potential slip surface with the driving forces arising principally from the self-weight of the structure. The soil mass bounded by the slip surface is divided

into vertical slices, for which force and moment equilibrium equations are established, and the factor of safety is defined as the ratio between available strength and mobilized demand. Methods differ in the assumptions adopted regarding interslice forces and the equilibrium conditions satisfied.

The Morgenstern-Price method, proposed by Morgenstern and Price (1965), is a general limit equilibrium method that simultaneously satisfies the three conditions of static equilibrium, namely force equilibrium in the horizontal and vertical directions and moment equilibrium, for slip surfaces of arbitrary shape, circular or otherwise. In this method, the relationship between the normal and shear forces acting on the interfaces between slices is expressed as $X = \lambda f(x) E$, in which $f(x)$ is an assumed interslice function, which may take forms such as constant or half-sine, and λ is a scale factor determined iteratively. The factor of safety and the parameter λ are obtained by simultaneous solution of the equilibrium equations, which confers greater rigour on the method relative to formulations that satisfy only part of these conditions, such as the Simplified Bishop method, which satisfies moment equilibrium alone. For this reason, and because of its applicability to surfaces of general shape, the Morgenstern-Price method is recognized as one of the most rigorous available and is the method adopted in the present work (Morgenstern and Price, 1965; Cheng and Lau, 2014; Duncan et al., 2014).

3. Materials and Methods

3.1 Overall structure

The study is organized in two methodologically complementary stages. Stage I comprises the development and application of a parametric procedure to assess the influence of the geometric parameters of iron ore tailings stacks on the factor of safety and on the storable volume, using reference geotechnical parameters compiled from the technical and scientific literature. Stage II comprises the application of the same methodology to an independent database, composed of topography and geotechnical parameters obtained from an operating mining project and determined through a laboratory testing programme. This organization allows both the geometric behaviour of the structure and the consistency of the method under different geotechnical conditions to be evaluated.

In both stages, three-dimensional modeling and volume calculation are performed in Micromine, and stability analyses are conducted in Slide2 (Rocscience) using the Morgenstern-Price method with automatic search for the critical slip surface. The three geometric parameters investigated are illustrated in Figure 1.

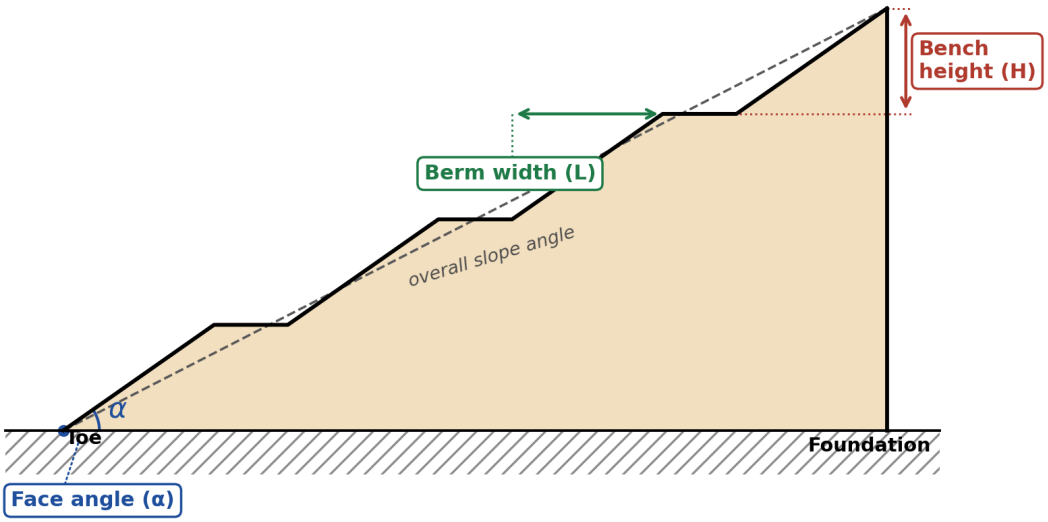

Figure 1. Schematic representation of the geometric parameters varied in the tailings stack models: face angle (α), berm width (L) and bench height (H).

3.2 Geometric modeling and volume estimation

Stage I uses a base topography obtained from a topographic survey of an area available for tailings disposal, bounded by a predefined physical limit polygon (Figure 2). The polygon represents the operational and physical constraints of the terrain that condition the implantation of the structure, and within which all evaluated geometric configurations are contained.

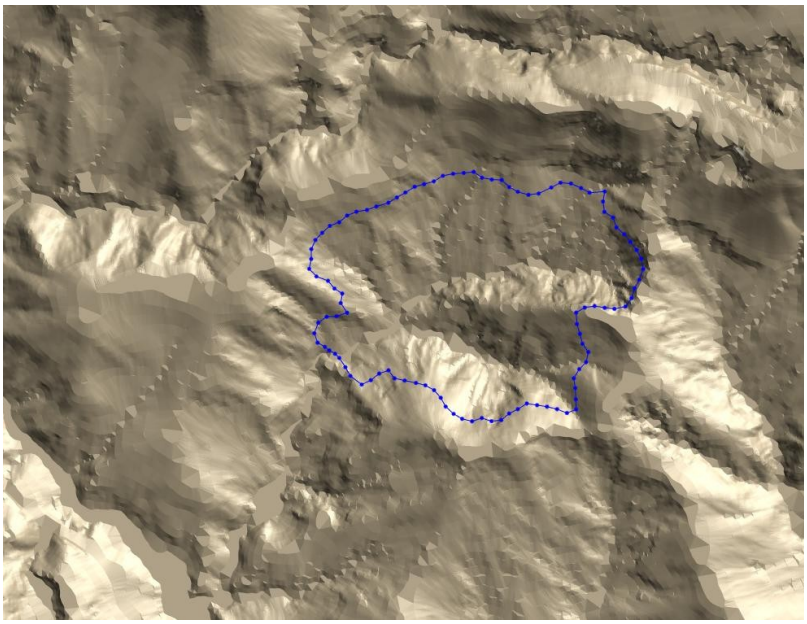

Figure 2. Physical limit polygon of the stack allocated on the Stage I base topography.

Three-dimensional modeling is executed in Micromine by means of the stack design tool, which builds the final surface of the structure from the base topography, the limit polygon and the geometric parameters defined for each scenario (Figure 3). The storable volume is computed as the difference between the modelled final surface and the original topography, and represents the effective disposal capacity of each evaluated configuration. To ensure maximum use of the available space, a deliberately high target volume is adopted as a design reference, so that the resulting geometry is conditioned

exclusively by the physical limit and by the defined geometric parameters, rather than by a volumetric restriction.

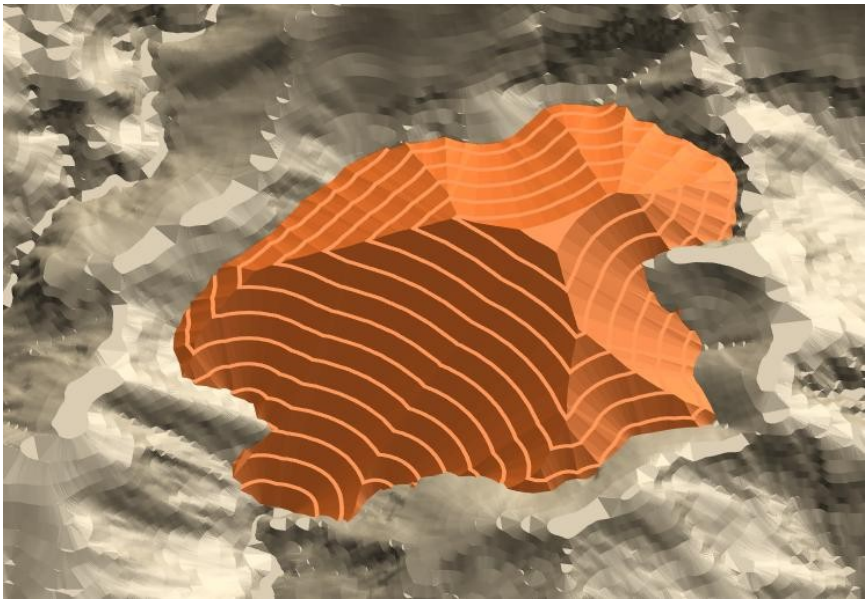

Figure 3. Three-dimensional model generated in Micromine.

From each three-dimensional model, cross-sections orthogonal to the direction of steepest slope of the stack are extracted (Figure 4). This criterion maximizes the probability of capturing the critical slip surface, since failures tend to develop in the regions of greatest gravitational demand (Duncan et al., 2014; Fontes et al., 2023). The factor of safety adopted for each configuration corresponds to the lowest value obtained among all analysed sections, a consolidated practice in geotechnical analyses of disposal structures (Duncan et al., 2014).

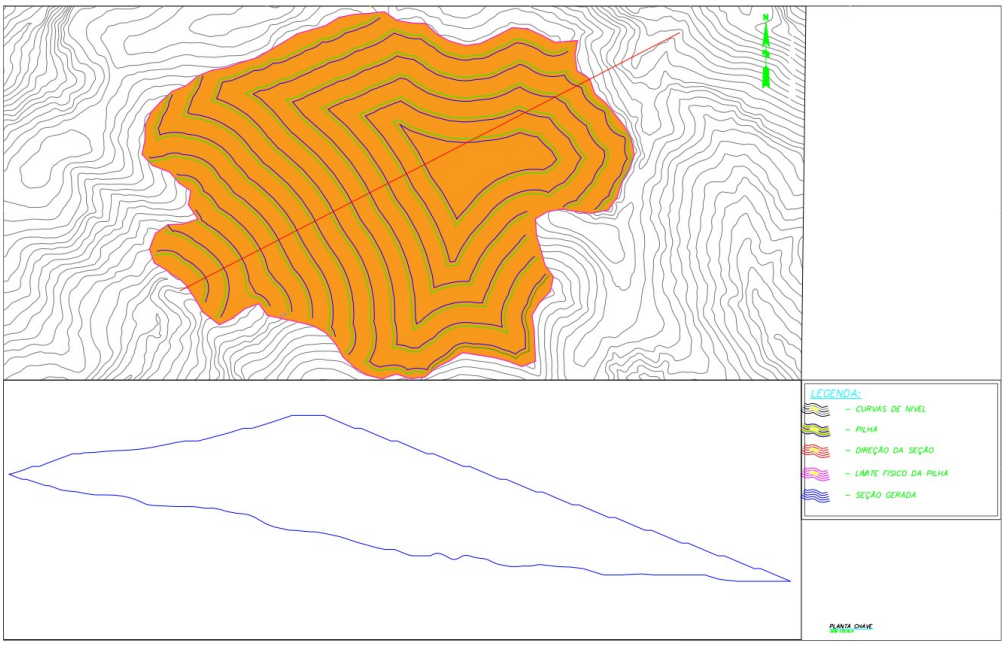

Figure 4. Example of a cross-section extracted orthogonally to the direction of steepest slope.

3.3 Parameter ranges

Analyses are conducted by varying one parameter at a time while keeping the others fixed at reference values, in a univariate sensitivity configuration. The three geometric parameters analysed and their

respective ranges of variation are: face angle (α), from 17° to 34° in increments of 0.5°; berm width (L), from 1.5 m to 10 m in increments of 0.25 m; and bench height (H), from 1.5 m to 12 m in increments varying between 0.25 m and 0.5 m according to the range of interest.

The reference values adopted for the parameters held fixed in each analysis series were as follows. In the face angle series, bench height and berm width were both fixed at 5 m. In the berm width and bench height series, the face angle was fixed at the normative limiting value, 23° in Stage I and 24° in Stage II, corresponding to the largest angle satisfying the FS ≥ 1.50 criterion. This limiting value was determined from the face angle sensitivity analysis itself (Section 4.1) and adopted as a reference in the remaining series, so that berm and height variations were evaluated under the most unfavourable admissible geometric condition, which confers a conservative character on the conclusions.

3.4 Stability analysis configuration

Stability analyses were conducted on representative two-dimensional sections with the objective of identifying the most critical failure condition for each geometric configuration. Analyses were performed under drained conditions, using strength parameters expressed in terms of effective stresses. This choice is founded on the characteristic geotechnical behaviour of filtered and compacted iron ore tailings, which exhibit relatively high permeability and low plasticity, favouring rapid dissipation of the pore pressures generated during construction (Fontes et al., 2023; Pereira, 2024). Under normal dry stacking operating conditions, the tailings are placed at a moisture content close to the compaction optimum and without saturation, so that the drained condition hypothesis adequately represents the in situ effective stress state (Ferrante et al., 2016; Barbosa, 2022).

The foundation is treated as a rigid, impermeable base, with no strength parameters assigned to an independent layer. This simplification is adopted intentionally to isolate the exclusive effect of geometric variations on the factor of safety, ensuring that comparisons between scenarios reflect only changes in inclination, bench height and berm width. The approach is consistent with established practice in parametric analyses of geometric sensitivity (Espósito, 2000; Cheng and Lau, 2014; Duncan et al., 2014). In detailed design, foundation strength must be investigated and incorporated into the model, since global slip surfaces may involve the substratum and result in factors of safety lower than those obtained with a rigid base, as demonstrated by Ferrante et al. (2016) in the analysis of Stack 2A.

Analyses were performed in Slide2 with the configuration parameters presented in Table 3. The Morgenstern-Price method was adopted with a half-sine interslice function (Morgenstern and Price, 1965). The number of slices was fixed at 25, the convergence tolerance at 0.005 and the maximum number of iterations at 50.

Table 3. Configuration parameters of the Slide2 stability analyses.

Parameter	Adopted value	Reference
Analysis method	Morgenstern-Price	Morgenstern and Price (1965)
Interslice function	Half-sine	Morgenstern and Price (1965)
Number of slices	25	Duncan et al. (2014)
Convergence tolerance	0.005	Cheng and Lau (2014)
Maximum iterations	50	Cheng and Lau (2014)
Surface type	Circular	Gerscovich (2016)
Search method	Auto Refine Search	Rocscience (2020)
Surfaces computed	4,500 per analysis	Rocscience (2020)

Parameter	Adopted value	Reference
Minimum slice width	0.5 m	Duncan et al. (2014)
Maximum base angle	70°	Duncan et al. (2014)
Check mα < 0.2	Active	Cheng and Lau (2014)

The search for slip surfaces was carried out by the Auto Refine Search method with circular surfaces, configured with 10 divisions along the slope, 10 circles per division and 10 refinement iterations, totalling 4,500 surfaces computed per analysis. The adoption of circular surfaces is consistent with the homogeneous nature of the material, since for masses with uniform properties the critical surface tends towards a circular shape (Gerscovich, 2016; Fontes et al., 2023). A minimum slice width of 0.5 m was enforced to avoid numerical instabilities associated with excessively thin slices (Duncan et al., 2014). The maximum slice base angle was limited to 70°, a value that eliminates surfaces with a basal inclination greater than twice the effective friction angle of the material ($\varphi' = 33°$), a physically unrealistic condition for cohesionless granular tailings, and prevents numerical instabilities associated with near-vertical slice bases (Duncan et al., 2014; Cheng and Lau, 2014; Rocscience, 2020). The verification criterion $m\alpha < 0.2$ was kept active, ensuring that slices with a negative or near-zero $m\alpha$ factor are flagged and preventing spurious convergence results characteristic of the Morgenstern-Price method (Cheng and Lau, 2014).

3.5 Stage II: independent database

Stage II applies the same parametric methodology to an independent database composed of topography and geotechnical parameters obtained from an operating iron ore project located in Minas Gerais. The base topography differs from that used in Stage I and reflects the actual terrain conditions of the project, with the stack implanted within a physical limit polygon likewise conditioned by local characteristics. This stage verifies whether the trends identified in Stage I are reproducible under different geotechnical and topographic conditions.

The geotechnical characterization adopted in Stage II was based on the laboratory tests performed by CI&A Lab (2022) on a sample of iron ore tailings representative of the material disposed in the field. Physical characterization indicated a specific gravity of solids of 3.348 g/cm³, a value that is high and consistent with the presence of iron-bearing particles. Combined grain size analysis, by sieving and sedimentation, showed a predominance of the fine fraction, with 95.1% of particles passing the 0.075 mm (No. 200) sieve, and the material was classified as a low-plasticity silt, with a liquid limit of 22%, a plastic limit of 18% and a plasticity index of 4%.

Shear strength was assessed by isotropically consolidated undrained triaxial compression tests on saturated specimens (CIUsat), performed on four specimens under confining stresses of 125, 250, 500 and 1000 kPa, with a Skempton B saturation parameter of 0.96. The maximum deviator stresses obtained were 319.0 kPa, 491.3 kPa, 825.8 kPa and 1318.0 kPa, respectively. The effective stress paths of the specimens are presented in Figure 5.

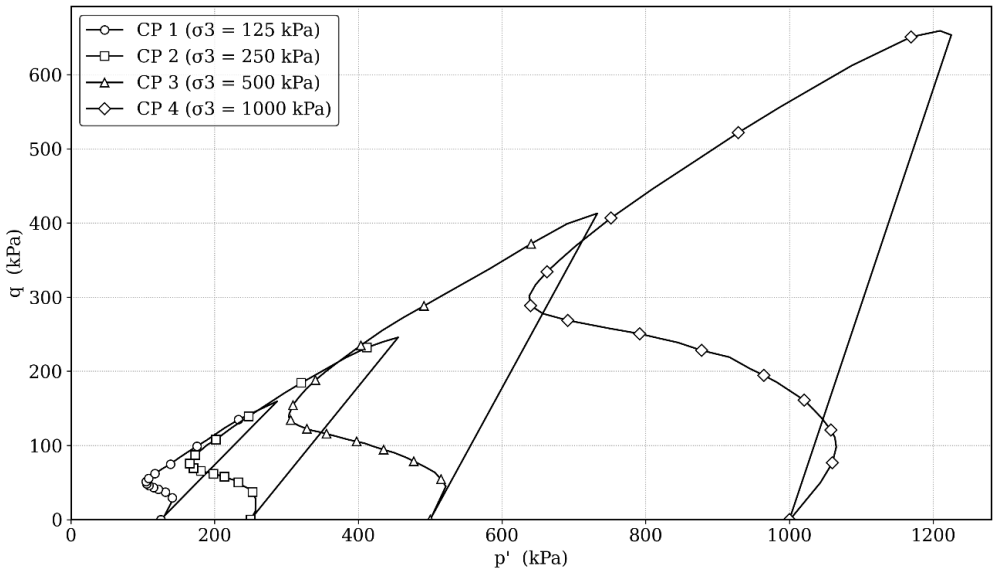

Figure 5. Effective stress paths of the specimens (CIUsat). Source: CI&A Lab (2022).

The effective strength envelope, drawn in p'-q space from the failure points, yielded an effective friction angle of 32°, as shown in Figure 6. Although the test indicated a small cohesion intercept, a null effective cohesion (c' = 0 kPa) was conservatively adopted in the stability analyses, together with the effective friction angle of 32°, the parameter that governs the strength of the material and to which the global factor of safety is directly sensitive.

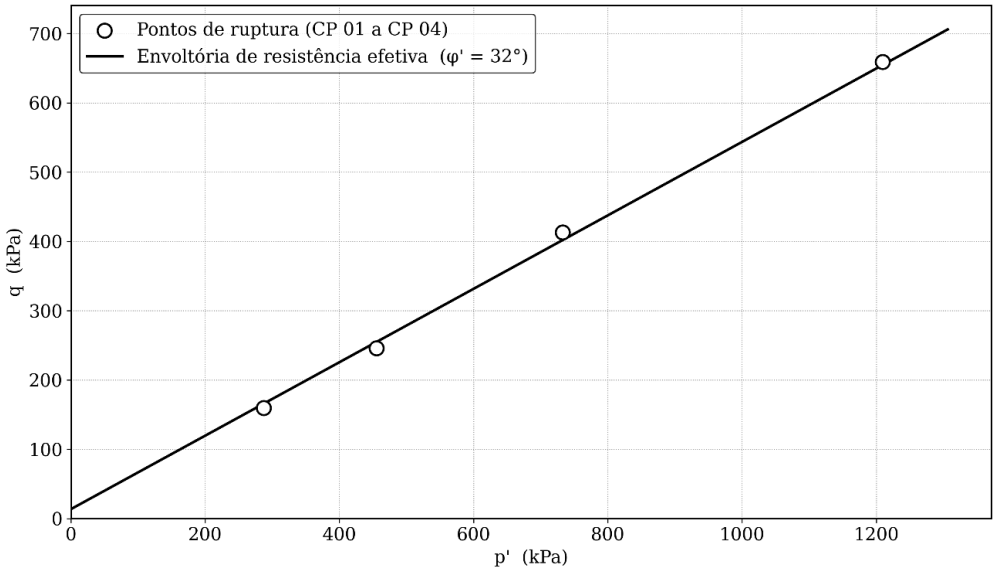

Figure 6. Effective strength envelope in p'-q space. Source: CI&A Lab (2022).

The bulk density of the soil obtained in the test was 2.02 g/cm³. Multiplied by the gravitational acceleration of 9.8 m/s², this results in the unit weight adopted for the tailings in the analyses, $\gamma = 9.8 \times 2.02 = 19.8$ kN/m³. The principal parameters of the geotechnical characterization are summarized in Table 4.

Table 4. Principal parameters of the Stage II geotechnical characterization (CI&A Lab, 2022).

Parameter	Value
Specific gravity of solids, ρs	3.348 g/cm³
Passing No. 200 sieve (0.075 mm)	95.1%

Parameter	Value
Liquid limit, LL	22%
Plastic limit, PL	18%
Plasticity index, PI	4%
Classification	Low-plasticity silt
Effective friction angle, φ'	32°
Adopted effective cohesion, c'	0 kPa (test indicated cohesion; adopted as null)
Bulk density obtained in the test, ρ	2.02 g/cm³
Unit weight, γ = 9.8 × 2.02	19.8 kN/m³

The Slide2 configuration used in Stage II is identical to that of Stage I in every aspect listed in Table 3, with the single distinction that the strength parameters entered in the model correspond to the values determined by CI&A Lab (2022). The analysis conditions (drained condition, rigid base, search criterion and numerical filters) remain unchanged, preserving comparability between stages.

The ranges of variation of the geometric parameters are based on those of Stage I, with the exception of the face angle, varied in increments of 1° in view of the number of scenarios already consolidated in Stage I. The Stage II analyses total 38 configurations distributed across the three families of parametric variation: 18 configurations for face angle (17° to 34°), 9 for berm width (2 m to 10 m) and 11 for bench height (2 m to 12 m). Since the density of sampling required to confirm an already known functional relationship is lower than that required to establish it originally, a deliberately smaller number of configurations was adopted, concentrated in the intervals and increments sufficient to reproduce the three relationships of interest.

4. Results and Discussion

Results are presented below, organized by the geometric parameter varied. For each parameter, the minimum factor of safety under drained conditions and the storable volume (Mm³ BCM) obtained in Stages I and II are reported, accompanied by a dual vertical axis plot and a table of complete results. The normative criterion adopted for the evaluation of stability is FS ≥ 1.50, as established by ABNT NBR 13028-3:2025.

4.1 Face angle

Figure 7 presents the FS and storable volume curves as a function of face angle (α) for Stages I and II. Table 5 compiles the complete numerical values of minimum FS and storable volume obtained in each analysis.

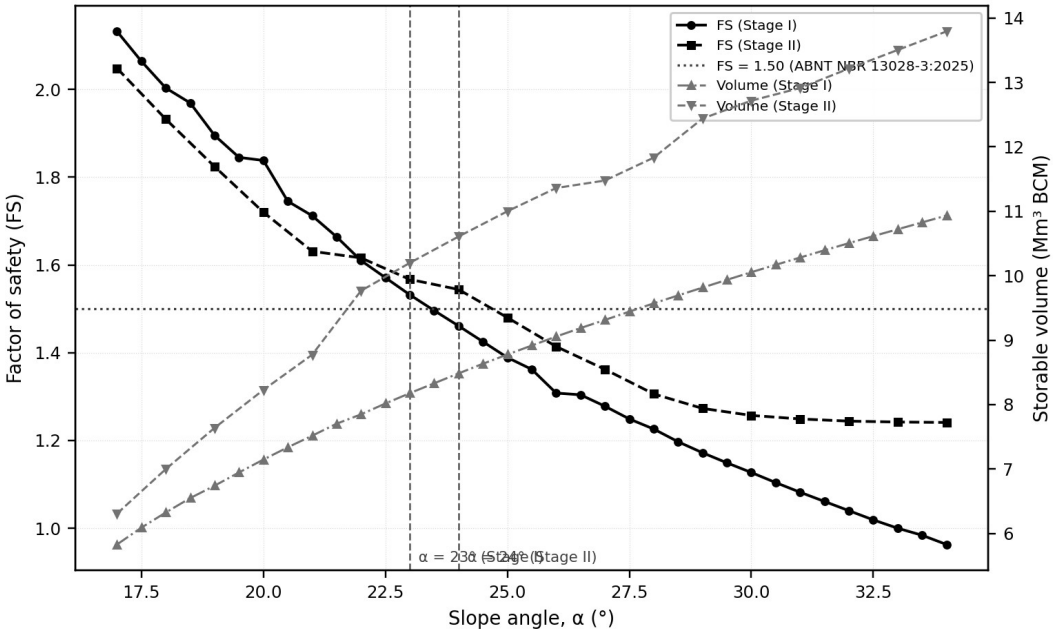

Figure 7. Factor of safety and storable volume as a function of face angle (α) for Stages I and II. Horizontal dotted line: FS = 1.50 (ABNT NBR 13028-3:2025). Vertical dashed lines: limiting angles of 23° (Stage I) and 24° (Stage II).

Table 5. Minimum factor of safety and storable volume by face angle (Stages I and II). Blank cells indicate angles not analysed in the corresponding stage.

α, Stage I (°)	Volume (Mm³ BCM)	FS (M-P)	α, Stage II (°)	Volume (Mm³ BCM)	FS (M-P)
17.0	5.829	2.132	17	6.308	2.048
17.5	6.090	2.064	18	7.000	1.932
18.0	6.326	2.003	19	7.639	1.824
18.5	6.549	1.969	20	8.228	1.720
19.0	6.741	1.895	21	8.775	1.631
19.5	6.947	1.845	22	9.766	1.616
20.0	7.147	1.838	23	10.199	1.567
20.5	7.337	1.745	24	10.608	1.544
21.0	7.517	1.712	25	11.000	1.480
21.5	7.703	1.664	26	11.361	1.414
22.0	7.848	1.610	27	11.477	1.362
22.5	8.017	1.571	28	11.832	1.306
23.0	8.177	1.532	29	12.439	1.273
23.5	8.331	1.496	30	12.716	1.257
24.0	8.484	1.461	31	12.912	1.249
24.5	8.634	1.425	32	13.214	1.244
25.0	8.777	1.389	33	13.503	1.242
25.5	8.916	1.362	34	13.791	1.241
26.0	9.056	1.308			
26.5	9.188	1.304			
27.0	9.314	1.278			

α, Stage I (°)	Volume (Mm³ BCM)	FS (M-P)	α, Stage II (°)	Volume (Mm³ BCM)	FS (M-P)
27.5	9.443	1.249			
28.0	9.571	1.226			
28.5	9.694	1.197			
29.0	9.815	1.172			
29.5	9.936	1.149			
30.0	10.054	1.127			
30.5	10.169	1.104			
31.0	10.282	1.082			
31.5	10.395	1.061			
32.0	10.505	1.040			
32.5	10.615	1.019			
33.0	10.720	1.000			
33.5	10.827	0.984			
34.0	10.933	0.963			

The variation of the face angle produced the most robust relationship of the entire study: FS decreases monotonically in both stages, with $R^2 = 0.969$ in Stage I and $R^2 = 0.916$ in Stage II. The linear regression for Stage I, $FS = -0.0666\,\alpha + 3.126$, indicates a loss of approximately 0.067 FS points per additional degree of inclination, whereas Stage II exhibits lower sensitivity, $FS = -0.0459\,\alpha + 2.668$. It should be stressed that both equations constitute empirical fits valid exclusively within the range of angles effectively analysed, from 17° to 34°, and for the specific topographic, geometric and geotechnical conditions of each stage; extrapolation beyond that interval or to other stack configurations is not recommended.

The limiting angle satisfying the FS ≥ 1.50 criterion of ABNT NBR 13028-3:2025 is 23° in Stage I (FS = 1.532) and 24° in Stage II (FS = 1.544). The transition from 17° to the limiting angle in Stage I represents a volumetric gain of +40.3%, from 5.83 to 8.18 Mm³ BCM, with no normative violation.

The practical significance of this behaviour is direct: operating close to the limiting angle is what makes storage capacity viable. The volumetric gain, however, is not linear with the angle. Because volume grows with inclination while FS decays approximately linearly, there exists a high-return interval in which each additional degree adds substantial volume while FS remains comfortably above 1.50, and the optimum lies precisely at the limiting angle, where the admissible volumetric gain is exhausted without normative violation. Any inclination below the limit represents wasted capacity, and any inclination above it is inadmissible, so that the limiting angle acts simultaneously as a safety ceiling and as a volumetric optimum. It must be noted, however, that the safety margin at this limit is narrow, lying a few percentage points above the minimum of 1.50, which implies a reduced reserve for uncertainties associated with the variability of strength parameters, partial saturation and construction surcharge. Operating at the volumetric optimum therefore demands rigorous control of these conditions throughout the service life of the structure.

This behaviour is consistent with established practice in disposal structures of the Iron Quadrangle. Barbosa (2022), performing two- and three-dimensional, deterministic and probabilistic stability analyses of a large filtered and compacted iron ore tailings stack in the same region, demonstrated the geotechnical viability of this type of structure when strength parameters are determined for different

degrees of compaction. Three-dimensional analyses tend to yield factors of safety higher than those of the equivalent two-dimensional sections, so that the 2D approach adopted in the present study is conservative. These results corroborate that filtered tailings stacks in the Iron Quadrangle designed with angles between 22° and 25° satisfy the normative criteria when strength parameters fall within the typical range compiled in Table 1.

4.2 Berm width

Figure 8 presents the FS and storable volume curves as a function of berm width (L), and Table 6 compiles the complete numerical values.

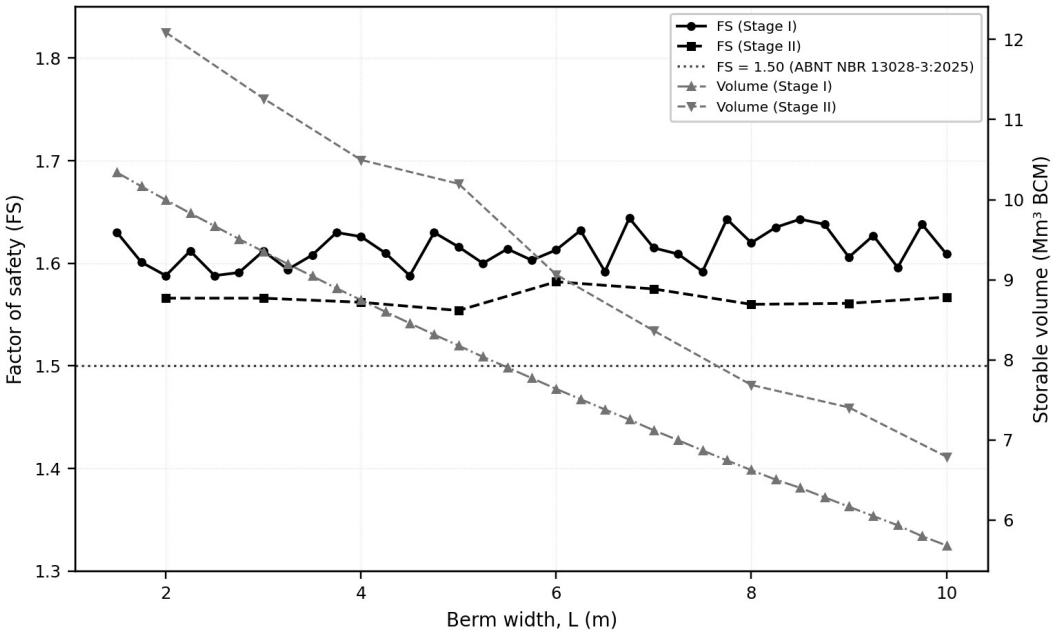

Figure 8. Factor of safety and storable volume as a function of berm width (L) for Stages I and II. Horizontal dotted line: FS = 1.50 (ABNT NBR 13028-3:2025).

Table 6. Minimum factor of safety and storable volume by berm width (Stages I and II).

L, Stage I (m)	Volume (Mm³ BCM)	FS (M-P)	L, Stage II (m)	Volume (Mm³ BCM)	FS (M-P)
1.50	10.339	1.630	2	12.088	1.566
1.75	10.165	1.601	3	11.264	1.566
2.00	9.997	1.588	4	10.496	1.562
2.25	9.831	1.612	5	10.199	1.554
2.50	9.670	1.588	6	9.065	1.582
2.75	9.509	1.591	7	8.364	1.575
3.00	9.352	1.612	8	7.687	1.560
3.25	9.196	1.594	9	7.406	1.561
3.50	9.045	1.608	10	6.790	1.567
3.75	8.893	1.630			
4.00	8.747	1.626			
4.25	8.601	1.610			
4.50	8.457	1.588			

L, Stage I (m)	Volume (Mm³ BCM)	FS (M-P)	L, Stage II (m)	Volume (Mm³ BCM)	FS (M-P)
4.75	8.315	1.630			
5.00	8.177	1.616			
5.25	8.037	1.600			
5.50	7.906	1.614			
5.75	7.772	1.603			
6.00	7.637	1.613			
6.25	7.509	1.632			
6.50	7.380	1.592			
6.75	7.254	1.644			
7.00	7.120	1.615			
7.25	6.997	1.609			
7.50	6.869	1.592			
7.75	6.744	1.643			
8.00	6.623	1.620			
8.25	6.504	1.635			
8.50	6.402	1.643			
8.75	6.284	1.638			
9.00	6.167	1.606			
9.25	6.050	1.627			
9.50	5.935	1.596			
9.75	5.798	1.638			
10.00	5.682	1.609			

The coefficient of variation of FS, only 1.07% in Stage I and 0.50% in Stage II across the entire range of widths analysed, constitutes the central quantitative evidence that the berm does not act as a control variable for global stability. Figure 8 illustrates this invariance: the FS curves of both stages are essentially horizontal, while the volume curves decrease linearly. The explanation lies in the identified failure mechanism. The critical surface develops within the individual bench face, confined between consecutive berms, and is therefore not intercepted by the berms and remains insensitive to their width. As noted by Duncan et al. (2014), the stabilizing effectiveness of intermediate geometric elements is conditional on their interaction with the critical slip surface; in the absence of that interaction, the berm is geometrically inert with respect to FS.

The volumetric cost, by contrast, is substantial: each additional metre of berm width eliminates 0.55 Mm³ of capacity in Stage I and 0.66 Mm³ in Stage II. Widening the berm from 1.5 m to 10 m in Stage I reduces the volume by 4.66 Mm³, equivalent to 45% of the capacity available at the optimum angle, with no stability return whatsoever. The resulting design directive is direct: berm width should be defined by the minimum operational criteria of access and surface drainage, and not by considerations of global stability.

4.3 Bench height

Figure 9 presents the FS and storable volume curves as a function of bench height (H), and Table 7 compiles the complete numerical values.

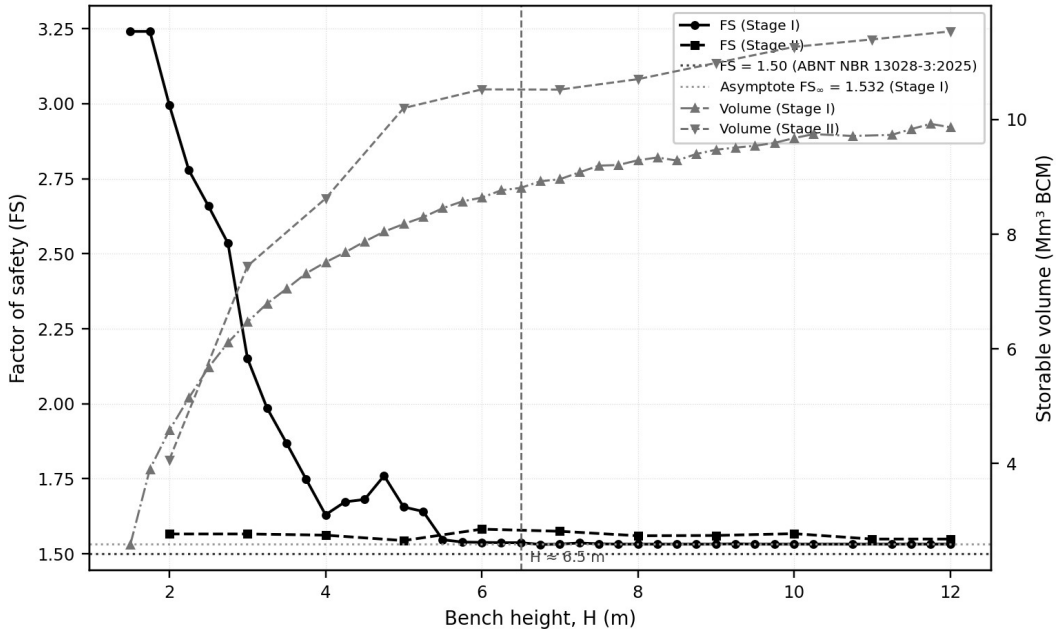

Figure 9. Factor of safety and storable volume as a function of bench height (H) for Stages I and II. Vertical dashed line: convergence threshold (H ≈ 6.5 m, Stage I). Horizontal grey dotted line: asymptote FS∞ = 1.532 (Stage I).

Table 7. Minimum factor of safety and storable volume by bench height (Stages I and II).

H, Stage I (m)	Volume (Mm³ BCM)	FS (M-P)	H, Stage II (m)	Volume (Mm³ BCM)	FS (M-P)
1.50	2.590	3.241	2	4.071	1.566
1.75	3.903	3.241	3	7.445	1.566
2.00	4.583	2.995	4	8.622	1.562
2.25	5.148	2.778	5	10.199	1.544
2.50	5.674	2.659	6	10.525	1.582
2.75	6.108	2.535	7	10.521	1.575
3.00	6.468	2.151	8	10.703	1.560
3.25	6.790	1.986	9	10.986	1.561
3.50	7.048	1.869	10	11.266	1.567
3.75	7.316	1.749	11	11.396	1.549
4.00	7.511	1.630	12	11.536	1.549
4.25	7.683	1.673			
4.50	7.872	1.681			
4.75	8.045	1.760			
5.00	8.177	1.656			
5.25	8.297	1.641			
5.50	8.452	1.547			
5.75	8.572	1.539			
6.00	8.638	1.538			
6.25	8.765	1.537			
6.50	8.808	1.537			
6.75	8.923	1.531			

H, Stage I (m)	Volume (Mm³ BCM)	FS (M-P)	H, Stage II (m)	Volume (Mm³ BCM)	FS (M-P)
7.00	8.959	1.532			
7.25	9.078	1.536			
7.50	9.195	1.533			
7.75	9.206	1.532			
8.00	9.289	1.532			
8.25	9.337	1.532			
8.50	9.285	1.532			
8.75	9.399	1.532			
9.00	9.472	1.532			
9.25	9.510	1.533			
9.50	9.542	1.532			
9.75	9.592	1.532			
10.00	9.676	1.532			
10.25	9.745	1.532			
10.75	9.714	1.532			
11.25	9.731	1.532			
11.50	9.832	1.532			
11.75	9.924	1.532			
12.00	9.865	1.532			

Stage I exhibited the geomechanically richest behaviour of the three parameters. For heights between 1.5 m and 2.75 m, FS is high (between 2.54 and 3.24), because the configuration is equivalent to a stack of many small steps with a gentle overall inclination. FS decreases up to H = 4 m and displays a non-monotonic interval between 4 m and 4.75 m, rising from 1.630 to 1.760 before returning to the descending trend, indicating a transition in the critical mechanism: the surface that crosses multiple benches, governing for smaller heights, gives way to the individual bench face mechanism, which prevails definitively beyond the convergence threshold.

From H ≈ 6.5 m onwards, FS converges asymptotically to 1.532, a value identical to that obtained in the angle series for α = 23°. This numerical coincidence is not fortuitous: it demonstrates that, above the convergence threshold, the critical surface develops within the individual bench face and FS is determined exclusively by the face inclination (α), becoming independent of bench height. Coutinho et al. (2024), in constructing a matrix of factors of safety for benches of iron mining disposal stacks with heights between 8 and 15 m and inclinations between 26° and 40°, using the Morgenstern-Price method, circular surfaces and Auto Refine Search in Slide2, operated entirely above this threshold, which explains why in that work FS responds primarily to the combination of angle and height within local bench mechanisms. The specific contribution of the present study is the precise identification of the transition threshold between the multiple-bench regime, which governs for reduced heights, and the individual bench face regime, an aspect not addressed by those authors.

For Stage II, the coefficient of variation of 0.69% confirms that the reference geometry already places the structure in the individual bench face regime from the outset of the variation. Volume grows by +281% in Stage I (from H = 1.5 m to 12 m) and by +183% in Stage II (from H = 2 m to 12 m), so that

maximizing bench height above the convergence threshold is the effective strategy for expanding capacity without any stability penalty.

4.4 Cross-stage comparison and synthesis

The one-degree difference in the limiting angle between the stages (23° against 24°) translates into a gain of 2.43 Mm³ at the optimum point of Stage II. The lower sensitivity to angle in Stage II (slope of −0.046 against −0.067) indicates that the real material is less penalized by increments of inclination, a behaviour attributable to the contribution of a non-null effective cohesion and to the higher unit weight of the tested tailings. This pattern is compatible with Fontes et al. (2023), who reported, for a filtered tailings co-disposal stack in Belo Horizonte with φ' = 31.5°, c' = 1.2 kPa and γ = 22.0 kN/m³, factors of safety close to the normative threshold in the critical sections, confirming that stacks with parameters in this range operate at narrow margins when the inclination approaches 23°. The present study quantifies those margins: FS is 0.032 above 1.50 at the optimum angle of Stage I and 0.044 at that of Stage II.

Figures 10 and 11 illustrate, by way of example, the critical slip surfaces obtained in Slide2 for the limiting angle geometries of each stage. In both cases, the critical surface identified by the Auto Refine Search develops within the individual bench face, confined between consecutive berms, without intercepting them. This configuration directly corroborates the numerical results of the three analysis families: the governing mechanism is that of the bench face, which explains the invariance of FS with respect to berm width and the asymptotic convergence observed in the bench height series.

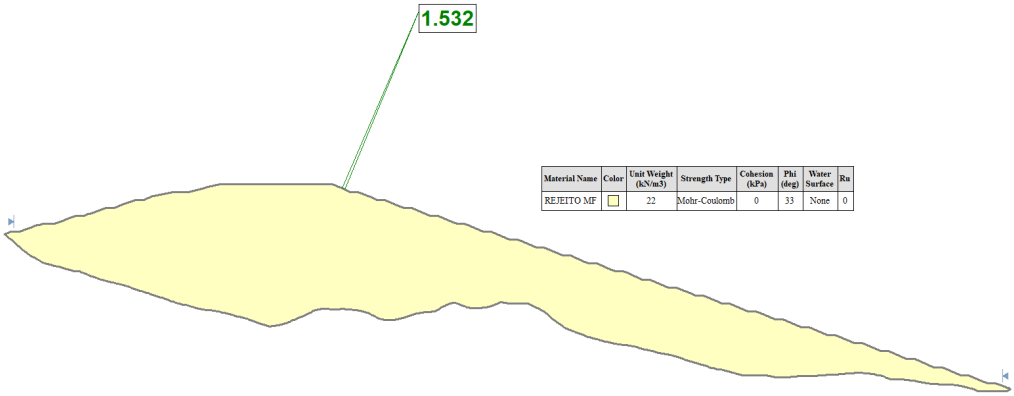

Figure 10. Critical slip surface obtained in Slide2 for the limiting angle geometry of Stage I (α = 23°, FS = 1.532), by the Morgenstern-Price method with Auto Refine Search.

Figure 11. Critical slip surface obtained in Slide2 for the limiting angle geometry of Stage II (α = 24°, FS = 1.544), by the Morgenstern-Price method with Auto Refine Search.

The convergence of the FS values obtained in the three analysis families for the same reference geometry internally validates the methodological consistency and supports the central conclusion of the work: the critical slip surface develops within the individual bench face and is governed exclusively by its inclination (α). The derived design directive is to fix the face angle at the normative limiting value, 23° for the Stage I parameters and 24° for those of Stage II, and to optimize berm width and bench height exclusively as a function of maximizing the storable volume within operational limits.

5. Conclusions

This work developed and applied a parametric analysis for the geometric optimization of dewatered iron ore tailings stacks, assessing the influence of face angle, berm width and bench height on the factor of safety and on the storable volume. The methodology was conducted in two stages: Stage I with reference parameters from the literature ($\varphi' = 33°$, $c' = 0$ kPa, $\gamma = 22$ kN/m³) and Stage II with parameters from laboratory tests (CI&A Lab, 2022) on tailings from an operating project. In both stages, three-dimensional modeling was executed in Micromine and stability analyses in Slide2 by the Morgenstern-Price method.

The face angle proved to be the geometric parameter governing the global factor of safety in both stages. The linear regressions obtained, $FS = -0.0666\,\alpha + 3.126$ (Stage I, $R^2 = 0.969$) and $FS = -0.0459\,\alpha + 2.668$ (Stage II, $R^2 = 0.916$), quantify the differential sensitivity between the parameter sets: each additional degree of inclination costs 0.067 FS points in Stage I and 0.046 in Stage II. These equations are valid strictly for the range of angles analysed, from 17° to 34°, and for the specific conditions of each stage, and should not be extrapolated. The limiting angle satisfying the $FS \geq 1.50$ criterion of ABNT NBR 13028-3:2025 is 23° in Stage I (FS = 1.532) and 24° in Stage II (FS = 1.544). Raising the angle from 17° to the normative limit in Stage I represents a volumetric gain of +40.3%, from 5.83 Mm³ BCM to 8.18 Mm³, which evidences the direct operational relevance of geometric optimization.

Berm width exerts no measurable influence on the global factor of safety. The coefficient of variation of FS was 1.07% in Stage I and 0.50% in Stage II across the entire range analysed (1.5 m to 10 m in Stage I and 2 m to 10 m in Stage II), confirming that the critical slip surface develops within the individual bench face without being intercepted by the berms. The volumetric cost of the berm, 0.55 Mm³ per additional metre in Stage I and 0.66 Mm³ in Stage II, indicates that its width should be defined exclusively by minimum operational criteria, without global stability considerations justifying larger values.

The bench height series revealed asymptotic behaviour in Stage I: the factor of safety decreases from 3.241 at H = 1.5 m and converges to 1.532 beyond $H \approx 6.5$ m, a value numerically identical to that obtained for $\alpha = 23°$ in the angle series. This coincidence demonstrates that, above the convergence threshold, the critical surface develops within the individual bench face and FS comes to be governed exclusively by the face inclination (α). The non-monotonic behaviour identified between H = 4 m and H = 4.75 m, with FS rising from 1.630 to 1.760, indicates a transition of the critical mechanism from the surface crossing multiple benches to that of the individual bench face within that range. In Stage II, the coefficient of variation of 0.69% across the entire range confirms that the individual bench face regime governs from the outset. The storable volume grows by +281% in Stage I from H = 1.5 m to 12 m, indicating that maximizing bench height above the threshold is the effective strategy for expanding capacity without any stability penalty.

The convergence of the factors of safety obtained across the three analysis families for the same reference geometry internally validates the methodological consistency and supports the central

conclusion of the work: the critical slip surface develops within the individual bench face, between consecutive berms, and is governed exclusively by the face inclination (α). The derived design directive consists of fixing the face angle at the normative limiting value (23° for the Stage I parameters and 24° for those of Stage II) and defining berm width and bench height, the latter above the convergence threshold, exclusively as a function of storable volume.

As a natural extension of this work, the incorporation of the foundation into the stability model as an independent layer is suggested, with its own strength and deformability parameters obtained from field and laboratory geotechnical investigation. The rigid, impermeable base hypothesis adopted in this study was intentional, with the purpose of isolating the exclusive effect of geometric variations on the factor of safety, but slip surfaces involving the substratum may result in factors of safety lower than those obtained with a rigid base, as demonstrated by Ferrante et al. (2016). A parametric analysis analogous to the one developed here, varying foundation stiffness and strength, would allow quantification of the conditions under which the limiting angle identified in this work ceases to be governed by the stack body and becomes conditioned by the founding terrain, including scenarios of an undrained foundation.

Comparison of the results obtained by the Morgenstern-Price method with other analysis methods is further recommended. Within limit equilibrium, alternative rigorous methods such as Spencer's, and simplified methods such as those of Bishop and Janbu, would allow the sensitivity of the factor of safety to the adopted interslice assumptions to be assessed (Cheng and Lau, 2014; Duncan et al., 2014). Complementarily, application of the shear strength reduction method in finite element analyses would dispense with the prior imposition of the shape of the slip surface, allowing independent verification of the individual bench face failure mechanism identified in this study. Finally, three-dimensional analyses, along the lines of those conducted by Barbosa (2022), would tend to yield factors of safety higher than those of the equivalent two-dimensional sections, so that their application would quantify the degree of conservatism embedded in the 2D approach adopted here and refine the limiting angle for design purposes.

Acknowledgements

The authors thank Thais Guimarães dos Santos for her supervision and technical guidance during the study on which this work is based. The authors also thank Micromine and, in particular, Jean Lacerda, for providing exclusive access to the Micromine software, which was essential to the completion of this work.

References

ABNT – Associação Brasileira de Normas Técnicas, 2025a. NBR 13028-1:2025. Mineração. Disposição de rejeitos. Parte 1: Terminologia. ABNT, Rio de Janeiro. (in Portuguese)

ABNT – Associação Brasileira de Normas Técnicas, 2025b. NBR 13028-2:2025. Mineração. Disposição de rejeitos. Parte 2: Requisitos para elaboração e apresentação de projetos. ABNT, Rio de Janeiro. (in Portuguese)

ABNT – Associação Brasileira de Normas Técnicas, 2025c. NBR 13028-3:2025. Mineração. Disposição de rejeitos desaguados em pilhas. ABNT, Rio de Janeiro. (in Portuguese)

Alves, P.I.A., 2020. Empilhamento de rejeito filtrado: a expansão de uma alternativa para substituição de barragens. MSc dissertation, Escola de Minas, Universidade Federal de Ouro Preto, Ouro Preto. (in Portuguese)

ANM – Agência Nacional de Mineração, 2020. Relatório Anual de Lavra: panorama da geração de rejeitos e estéreis de mineração 2010–2019. ANM, Brasília. (in Portuguese)

ANM – Agência Nacional de Mineração, 2022. Resolução ANM nº 95, de 07 de fevereiro de 2022. ANM, Brasília. (in Portuguese)

ANM – Agência Nacional de Mineração, 2024. Anuário Mineral Brasileiro 2024. ANM, Brasília. (in Portuguese)

Barbosa, C.V., 2022. Análise de estabilidade tridimensional e bidimensional em uma pilha de rejeito filtrado de grandes dimensões. MSc dissertation, Universidade Federal de Viçosa, Viçosa. https://doi.org/10.47328/ufvbbt.2022.620 (in Portuguese)

Brasil, 2020. Lei nº 14.066, de 30 de setembro de 2020. Altera a Lei nº 12.334/2010, Política Nacional de Segurança de Barragens. Diário Oficial da União, Brasília. (in Portuguese)

Carmignano, O.R.D.R., Lago, R.M., Santos, U.P., 2023. Processos de inovação em rede como uma estratégia para a destinação de rejeitos da mineração de ferro: o caso da Plataforma R3 Mineral. Revista Brasileira de Inovação 22, e023001. https://doi.org/10.20396/rbi.v22i00.8664705 (in Portuguese)

Carvalho, J.V.A., et al., 2024. On the behavior of compacted filtered iron ore tailings. In: IS-Porto 2024, International Symposium on Geotechnics of Mine Waste. E3S Web of Conferences 544. https://doi.org/10.1051/e3sconf/202454413004

Cheng, Y.M., Lau, C.K., 2014. Slope Stability Analysis and Stabilization: New Methods and Insight, 2nd ed. CRC Press, New York.

CI&A Lab, 2022. Relatório de ensaios de caracterização geotécnica de rejeito filtrado de minério de ferro. Technical report. (in Portuguese)

Coelho, P., Camacho, D., 2024. The experimental characterization of iron ore tailings from a geotechnical perspective. Applied Sciences 14 (12), 5033. https://doi.org/10.3390/app14125033

Consoli, N.C., et al., 2022. Behaviour of compacted filtered iron ore tailings–Portland cement blends: new Brazilian trend for tailings disposal by stacking. Applied Sciences 12 (2), 836. https://doi.org/10.3390/app12020836

Coutinho, A., Coelho, G., Meireles, L., 2024. Uso de mapa de fator de segurança durante a operação de pilhas de rejeito e estéril. In: 17th Pan-American Conference on Soil Mechanics and Geotechnical Engineering (XVII PCSMGE), La Serena. ISSMGE. (in Portuguese)

Davies, M., 2011. Filtered tailings, the fundamentals. In: Tailings and Mine Waste 2011. Norman B. Keevil Institute of Mining Engineering, Vancouver.

Duncan, J.M., Wright, S.G., Brandon, T.L., 2014. Soil Strength and Slope Stability, 2nd ed. John Wiley & Sons, Hoboken.

Espósito, T.J., 2000. Metodologia probabilística e observacional aplicada a barragens de rejeito construídas por aterro hidráulico. PhD thesis, Universidade de Brasília, Brasília. (in Portuguese)

Ferrante, F., Aguiar, M.F.P., Carvalho, E.P., Cota, F.L.D.G., 2016. Análise de estabilidade de pilha de rejeito de minério de ferro. In: XVIII Congresso Brasileiro de Mecânica dos Solos e Engenharia Geotécnica, COBRAMSEG 2016. ABMS, Belo Horizonte. (in Portuguese)

Fontes, M.M.M., et al., 2023. Comparative analysis of the effect of disposal in tailings and waste rock piles. In: Tailings and Mine Waste Conference, TMIC 2022. Advances in Hazardous, Environmental and Energy Engineering 13, 29–43. https://doi.org/10.2991/978-94-6463-104-3_4

Fourie, A.B., 2012. Perceived and realized benefits of paste and filtered tailings for surface deposition. In: Jewell, R.J., Fourie, A.B. (Eds.), Paste 2012. Australian Centre for Geomechanics, Perth.

Fredlund, D.G., Rahardjo, H., 1993. Soil Mechanics for Unsaturated Soils. John Wiley & Sons, New York.

Gerscovich, D.M.S., 2016. Estabilidade de Taludes, 2nd ed. Oficina de Textos, São Paulo. (in Portuguese)

Guimarães, N.C., 2011. Filtragem de rejeitos de minério de ferro visando à sua disposição em pilhas. MSc dissertation, Universidade Federal de Minas Gerais, Belo Horizonte. (in Portuguese)

Hernandez, H.M.O., 2002. Caracterização geomecânica de rejeitos aplicada a barragens de aterro hidráulico. MSc dissertation, Universidade de Brasília, Brasília. (in Portuguese)

IBRAM – Instituto Brasileiro de Mineração, 2023. Relatório Anual da Mineração no Brasil 2023. IBRAM, Brasília. (in Portuguese)

IBRAM – Instituto Brasileiro de Mineração, 2024. Mineração em Números 2024. IBRAM, Brasília. (in Portuguese)

Lopes, R.L., 2000. Caracterização geotécnica de rejeitos de beneficiamento de minério de ferro. MSc dissertation, Universidade Federal de Viçosa, Viçosa. (in Portuguese)

Morgenstern, N.R., Price, V.E., 1965. The analysis of the stability of general slip surfaces. Géotechnique 15 (1), 79–93.

Morgenstern, N.R., et al., 2016. Report on the immediate causes of the failure of the Fundão dam. Fundão Tailings Dam Review Panel.

Pereira, L.M.M. (Lucas Mazullo Mascarenhas Pereira), 2024. Estudo de propriedades geotécnicas de um rejeito de minério de ferro filtrado compactado para empilhamento a seco. MSc dissertation, Escola Politécnica, Universidade de São Paulo, São Paulo. (in Portuguese)

Presotti, E.S., 2002. Influência do teor de ferro nos parâmetros de resistência de um rejeito de minério de ferro. MSc dissertation, Escola de Minas, Universidade Federal de Ouro Preto, Ouro Preto. (in Portuguese)

Rocscience, 2020. Slide2 User Guide. Rocscience Inc., Toronto.

Wickland, B.E., Wilson, G.W., Wijewickreme, D., Klein, B., 2006. Design and evaluation of mixtures of mine waste rock and tailings. Canadian Geotechnical Journal 43 (9), 928–945.